Microstructural characterization of proton-irradiated type 316 stainless steel

Yun Soo Lim*, Seong Sik Hwang, Dong Jin Kim, Min Jae Choi, Jong Yeon Lee
Nuclear Materials Safety Research Division/Korea Atomic Energy Research Institute
1045 Daedeok-daero, Yuseong-gu, Daejeon 305-353, Korea
**Corresponding author: yslim@kaeri.re.kr*

1. Introduction

Irradiation-assisted stress corrosion cracking (IASCC) of internal components of a pressurized water reactor (PWR) is considered critical for safe long-term operation. Some cracking of internals made of stainless steel (SS), such as guide tube support pins, baffle former bolts and so on, has been identified [1]. The IASCC mechanism is not fully understood; however, it appears to be closely related to microstructural defects caused by neutron irradiation. Therefore, studies on microstructural changes should be the first step to understand how irradiation defects affect the cracking behavior of these alloys. Proton irradiation is a useful experimental technique to study irradiation-induced phenomena in nuclear core materials instead of neutrons [2]. Under the proper irradiation conditions, proton irradiation can produce a microstructure and microchemistry very similar to that of neutron irradiation. The challenging issue is that proton irradiation-induced defects accumulate near the surface within a narrow range of a few tens of micrometers, with the level of radiation damage changing sensitively depending on the depth. The objectives of the present work were to investigate the irradiation defects depending on the irradiation depth and radiation dose using transmission electron microscopy (TEM) in the proton-irradiated 316 austenitic SS and to discuss their influence on IASCC.

2. Methods and Results

2.1 Material and Proton Irradiation

Type 316 austenitic SS was used in this study. The chemical composition of the alloy is given in Tables 1.

Table 1. Composition of the 316 austenitic SS (wt%)

Cr	Ni	C	Mo	Mn	Si	Cu	P	Fe
16.1	10.4	0.047	2.11	1.08	0.66	0.1	0.003	Bal.

The test alloy was solution annealed at 1100 ℃ and finally water quenched. Before the proton irradiation, the surfaces of the specimens were mechanically ground and then electrochemically polished in a solution of 50 vol% phosphoric acid + 25 vol% sulfuric acid + 25 vol% glycerol for 15 - 30 s at room temperature. The proton irradiation was performed with the General Ionex Tandetron accelerator at the Michigan Ion Beam Laboratory at the University of Michigan. The irradiation processes were conducted using 2.0 MeV protons at a current range of 40 ㎂. Details of the irradiation procedure can be found in the literature [3]. The specimens were exposed at 360 ℃ to four levels of irradiation of 0.4, 1.6, 2.7, and 4.2 displacements per atom (dpa) at a depth of 15 ㎛ from the surface, which will be referred as A, B, C and D specimens hereafter. The radiation damage levels of the samples were calculated with the Stopping and Range of Ions in Matter (SRIM) program using a displacement energy of 40 eV in the 'quick calculation' mode.

2.2 Sample Preparation and Microstructural Analysis

The specimens for optical microscopy and SEM were prepared by chemical etching in a solution of 2 vol% bromine+98 vol% methanol. TEM foils containing the irradiated area were prepared with conventional electro-polishing (EP) method. To prepare the TEM specimens, thin foils were mechanically thinned until they were less than 40 ㎛ thick and then electro-jet polished in a 7 vol% perchloric acid + 93 vol% methanol solution at -40 ℃ with a current of approximately 80 mA.

The FIB TEM specimens of the proton-irradiated 316 SS were prepared using a dual-beam Hitachi FIB-2100 system with Ga ions with an incident beam energy level of 30 kV and a current of 1 – 5 nA. Final thinning was done at an acceleration voltage of 5 kV to eliminate the surface damage produced by highly energetic ions in the early stage of the FIB milling process. The chemical polishing (CP) of the FIB TEM specimens was done in a slowly stirred solution of 0.5 vol% Br + 99.5 vol% methyl alcohol for 15 s at room temperature to remove completely the surface defects produced during the FIB TEM fabrication process.

The proton-irradiated specimens were investigated using various types of microscopic equipment. The SEM imaging and orientation imaging microscopy by electron back-scattered diffraction (EBSD) were done with a JEOL 5200 (operating voltage 25 kV) and a JEOL 6300 (operating voltage 20 kV), respectively. TEM analysis was done with a JEOL JEM-2100F (operating voltage 200 kV) to determine the typical microstructural changes due to proton irradiation.

2.3 TEM Results on the Irradiation Defects

The irradiation damages depending on the dpa and the depth of 316 SS were calculated with the Stopping

and Range of Ions in Matter (SRIM) 2008 program using a displacement energy of 40 eV in the 'quick calculation' mode. These results are given in Fig. 1. The damage profiles exhibit a slow increase roughly up to a depth of 15 ㎛, as well as subsequent damage peaks near the depth of 20 ㎛ from the irradiated surfaces.

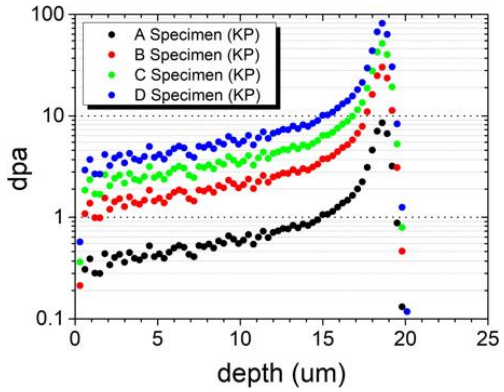

Fig. 1. Calculated dpa-depth profiles of the proton-irradiated 316 SS using the 'quick calculation' mode of SRIM program.

Fig. 2 shows a typical dislocation morphology in the as-received type 316 SS obtained from an EP treatment before proton irradiation. The dislocation density was quite low due to the high-temperature solution-annealing treatment of 1100 ℃, and the dislocations appeared to be in a straight form. The type 316 SS has a low stacking fault energy; therefore, images due to stacking faults are frequently observed in such specimens as shown in Fig. 2.

Fig. 2. TEM image showing a dislocation morphology in the non-irradiated 316 SS.

Fig. 3 shows dislocations and point defects observed in an area of the FIB and then CP-treated specimen after proton irradiation with a radiation dose of 1.6 dpa at a depth of ~ 16 ㎛ from the surface of A specimen. The dislocation density was increased considerably by proton irradiation, compared to the density levels in the non-irradiated specimens shown in Fig. 2. An increase in the dislocation density depending on the proton radiation dose was also confirmed in Ni-based Alloy 600 [4].

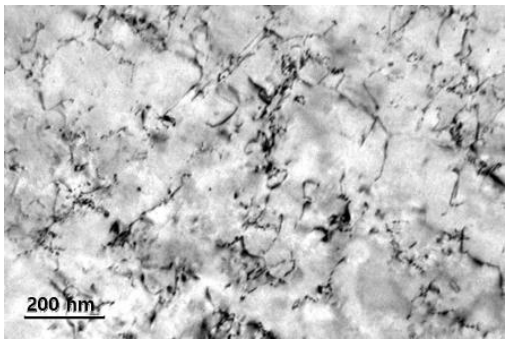

Fig. 3. TEM image showing a dislocation morphology in the proton-irradiated 316 SS with a dose of 1.6 dpa.

Fig. 4 is a TEM image showing the micro-voids found in the proton-irradiated specimen. The observation depth of the TEM specimen was ~18 ㎛ from the surface of B specimen, which means that the irradiation dose was approximately 30 dpa at this depth (Fig. 1). Fig. 4 was obtained in the under-focus condition, from which the image of the voids could be visualized clearly. On the other hand, voids were not found in the specimens which contained areas with the radiation dose less than 2 dpa. All of these results imply that there is a threshold dpa at which voids can be generated. The average size and the number density of the voids increased as the radiation dose increased. Other researchers also have reported that voids are rarely generated below a certain radiation dose for a given material [5,6], and Sencer et al. [6] have found that the number density of the voids gradually increases as the radiation dose is increased.

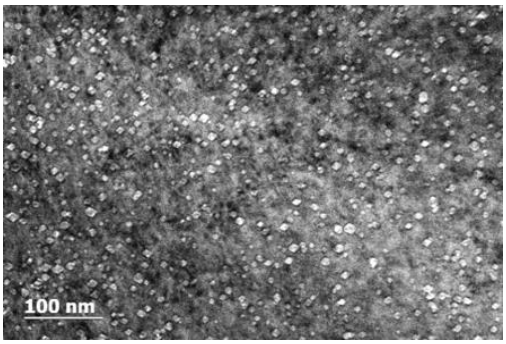

Fig. 4. TEM bright field image showing micro-voids in the 316 SS proton-irradiated to approximately 30 dpa.

The density of the network dislocations also increased considerably by proton irradiation, and the degree of increase seemed to depend on the dose of the proton irradiation. All the present findings are in good agreement with the previously reported results on neutron and proton-irradiated stainless steels.

2.4 Effects of Irradiation on IASCC

The characteristics of microscopic changes by irradiation and their role in changes of material behavior and IASCC have been extensively studied [7]. Irradiation of a material causes hardening, radiation-induced segregation (RIS) and localized deformation. Radiation-induced hardening basically originates from the introduction of a large amount of small Frank loops and network dislocations (Fig. 3) in the material, which increases the yield stress and lowers the fracture toughness. Uniform elongation is also reduced sharply when a material is irradiated. As such, the alloy becomes significantly embrittled in the PWR operation condition, which in turn makes it much more susceptible to IASCC by irradiation.

RIS leads to the changes in the grain boundary composition. It was found from our previous study that Cr, Mo and Mn were depleted at the grain boundary, while Ni, Si, B and P were enriched. It was also reported that Cr depletion at the grain boundaries was closely correlated with component failures [8], which is a phenomenon very similar to that Cr depletion at the grain boundaries in austenitic alloys due to thermal sensitization as the main cause of intergranular cracking. Fig. 5 shows the effect of proton irradiation on the crack growth rates (CGRs) of the solution-annealed and sensitized type 304 SS depending on the dpa value. From the figure, it can be confirmed that proton irradiation increases considerably the CGRs of the solution-annealed type 304 SS due to the irradiation-induced Cr depletion at the grain boundaries.

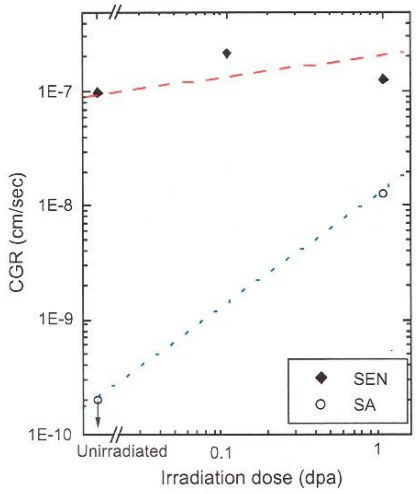

Fig. 5. The effect of proton irradiation on the CGRs of solution-annealed and sensitized type 304 SS in a function of the dpa values [8].

Another factor playing an important role in IASCC is localized deformation. The formation of intense deformation channels that transmit dislocations to the grain boundaries can result in localized slip or sliding of the grain boundary and cause the initiation of intergranular cracks. As a result, the combined effect of hardening, RIS and localized deformation by irradiation can significantly reduce the resistance to IASCC of a structural material under irradiation.

3. Conclusions

Type 316 SS samples were irradiated using 2 MeV protons with an average dose rate of ~7.1 x 10^{-6} dpa/s at 360 ℃, and the various defects generated by proton irradiation were characterized using CP-treated FIB TEM specimens. The types of irradiation damage examined were point defects, dislocations and voids. Point defects and dislocations were found mainly in the area exposed to a low radiation dose; however, voids were dominant in areas exposed to a high radiation dose. Consequently, the evolution of typical irradiation defects differs with the depth, in good agreement with the characteristics of the radiation damage profile depending on the depth. This behavior is considered to be a general characteristic of any type of ion irradiation. All of the microstructural and microchemical changes induced by irradiation degrade the mechanical properties of a material and significantly reduce the resistance to IASCC of structural components installed near the core region of a PWR.

REFERENCES

[1] J. McKinley, R. Lott, B. Hall and K. Kalchik, Examination of Baffle-Former Bolts from D.C. Cook Unit 2, Proc. of the 16th Int. Conf. on Environmental Degradation of Materials in Nuclear Power Systems-Water Reactor, 2013.
[2] J. Gan and G.S. Was, Microstructure Evolution in Austenitic Fe-Cr-Ni Alloys Irradiated with Rotons: Comparison with Neutron-Irradiated Microstructures, Journal of Nuclear Materials, Vol.297, p. 161, 2001.
[3] G.S. Was, J.T. Busby, T. Allen, E.A. Kenik, A. Jenssen, S.M. Bruemmer, J.Gan, A.D. Edwards, P.M. Scott and P.L. Andresen, Emulation of Neutron Irradiation Effects with Protons: Validation of Principle, Journal of Nuclear Materials, Vol.300, p. 198, 2002.
[4] J.-J. Kai and R.D. Lee, Effects of proton irradiation on the microstructural and microchemical evolution of Inconel 600 alloy, Journal of Nuclear Materials, Vol.207, p.286, 1993.
[5] Z. Jiao, J.T. Busby, G.S. Was, Deformation microstructure of proton-irradiated stainless steels, Journal of Nuclear Materials, Vol.361, p. 218, 2007.
[6] B.L. Sencer, G.S. Was, M. Sagisaka, Y. Isobe, G.M. Bond, F.A. Garner, Proton irradiation emulation of PWR neutron damage microstructures in solution annealed 304 and cold-worked 316 stainless steels, Journal of Nuclear Materials, Vol.323, p. 18, 2003.
[7] G.S. Was, S.M. Bruemmer, Effects of Irradiation on Intergranular Stress Corrosion Cracking, Journal of Nuclear Materials, Vol.216, p. 326, 1994.
[8] L.H. Wang, C.H. Tsai, J.J. Kai, Effect of prior thermal treatment on the microchemistry and crack propagation of proton-irradiated AISI 304 stainless steels, Journal of Nuclear Materials, Vol.328, p. 11, 2004.